UNIVERSITY OF WATERLOO

ME 362
Fluid Dynamics II

W25 Term Project
Professor Devaud

Analyzing the Theoretical Trajectory and Contribution of Magnus Force and Drag to 2023-2024 MLB Season Pitches

Members:

Miklos Balogh - 20976832
Alicia Ng - 20832882
Artem Ovsyannikov - 20910644
Arianna Rauliuk - 20889357
Alan Su - 20844214

Submission Date:
April 4th, 2025

1. Table of Contents

2. Table of Figures

3. Table of Tables

4. Table of Equations

5. Historical Development and Pertinent Developments in the State of Baseball

Commented [MB1]: Good Enough

Baseball has long been recognized as a defining element of American culture, often earning the title of the country's unofficial national sport. While the game's exact beginnings are still debated, most historians agree that it originated from bat-and-ball games played in England during the 18th century. These games eventually made their way to North America, where they evolved into the sport we now recognize as baseball.

The earliest officially recorded baseball game in the United States took place in 1846 in Hoboken, New Jersey. From that point forward, the sport rapidly grew in popularity throughout the country. During its early development, different regions followed varying sets of rules and used a range of equipment, reflecting baseball's evolving nature. In 1876, the National League was established, marking the birth of professional baseball in the U.S. This milestone led to the formation of other leagues, most notably the American League in 1901. These two major organizations eventually united under the banner of Major League Baseball (MLB), with the merger becoming official in 2000.

As the sport developed, so too did the techniques and strategies employed by pitchers, leading to the evolution of a wide variety of pitch types, each designed to challenge hitters in unique ways. Among the most fundamental are the four-seam fastball and curveball. The four-seam fastball is the most frequently utilized and typically the fastest pitch in a pitcher's repertoire. Thrown with a grip that maximizes true backspin, it exhibits minimal lateral deviation and a relatively straight trajectory, while appearing to 'rise' from the perspective of a batter.

From a fluid mechanics perspective, the high backspin generates a significant upward Magnus force, which counteracts gravitational acceleration. This lift effect results in reduced vertical drop, producing what is perceptually described as a "rising" fastball, although the pitch still descends physically. The pitch derives its name from the fact that four seams are visible with each rotation when thrown correctly. It is generally released with uniform finger pressure and a clean backspin axis, which stabilizes the pitch and reduces turbulent wake asymmetry.

The high velocity of the pitch reduces the time available for gravitational and aerodynamic forces to act, further limiting its drop and horizontal deviation.

The curveball is a breaking pitch, characterized by significant vertical and often horizontal deviation. It is thrown at a reduced velocity relative to fastballs and relies on topspin to produce an exaggerated downward Magnus force. The Magnus effect causes air to accelerate over the top of the ball and decelerate underneath it, leading to a net downward aerodynamic force that adds to gravitational drop. The diversity of break patterns is governed by the orientation of the spin axis, which defines the direction and

magnitude of the Magnus force. A properly executed curveball will sharply deviate from the expected fastball trajectory, leading to mis-aimed swings. However, when insufficient spin or misaligned release occurs, the pitch may fail to break, resulting in a “hanging” curveball that is easier for batters to hit.

In baseball, pitch movement is a crucial factor that influences the effectiveness of a pitch. This movement results from a combination of gravitational forces and the interactions between the spinning baseball and the surrounding air. Two common terms used to qualitatively describe pitch movement are “drop in” (vertical component) and “break in” (horizontal component). "Drop in" refers to the downward vertical displacement of a pitch as it travels toward home plate. It is typically caused by gravitational acceleration and the absence or presence of upward lift. From a fluid dynamics standpoint, the vertical movement of a pitch is influenced by both gravity and the Magnus effect, where the spin of the ball alters the pressure distribution around its surface.

In a pitch such as a curveball, topspin increases the downward Magnus force, amplifying the "drop." Conversely, a four-seam fastball with high backspin generates upward Magnus force, counteracting gravity and resulting in less vertical drop, or a "rising" effect (though it still physically descends). "Break in" refers to the lateral (sideways) movement of a pitch toward the batter’s body (for same-handed matchups) or away from it (for opposite-handed matchups), depending on the pitch type and spin direction. This horizontal movement creates an asymmetric pressure field due to the Magnus effect. The side of the ball spinning against the direction of travel experiences higher pressure, while the side spinning with the travel direction experiences lower pressure, resulting in a net lateral force. For example, a two-seam fastball or a slider with arm-side spin will "break in" toward the same side as the pitcher’s throwing hand. The “break in” and “drop in” will be examined in this report. They will be calculated using factors that affect the pitch of a baseball, provided by statistics from the official MLB page.

Besides Pitch Type (Fastball, Curveball), and Axis (Four-Seam vs. Two-Seam Fastballs), other factors also affect the Break In and Drop In. These include Velocity (VELO), Angular Velocity/Spin Rate (SR), Extension (EXT). These variables influence the generation and magnitude of lift and lateral forces through mechanisms such as the Magnus effect, drag, and the pressure gradient surrounding the spinning ball.

Velocity (VELO) plays a fundamental role in determining the influence of both gravity and aerodynamic forces on the ball. From a fluid mechanics perspective, velocity affects the Reynolds number, which characterizes the flow regime around the ball and influences the wake structure. Higher velocity reduces the amount of time gravity and Magnus forces can act on the ball before it reaches home plate, thereby reducing both vertical drop and lateral break. Additionally, faster pitches experience greater dynamic pressure, intensifying the aerodynamic lift generated by spin. Spin Rate (SR) refers to the angular velocity of the baseball and directly affects the magnitude of the Magnus force, a lift force resulting from

pressure differentials created by the interaction of the ball's surface spin with surrounding air. A higher spin rate increases the asymmetry of airflow, enhancing lift (in the case of backspin) or downward force (in the case of topspin). For example, a fastball with high backspin generates upward Magnus force that counteracts gravity, reducing vertical drop. In contrast, a curveball with high topspin increases the downward Magnus force, leading to enhanced drop. Extension (EXT) reduces the effective flight time of the pitch, limiting the window during which gravity and Magnus forces can influence the ball's trajectory. In essence, greater extension shortens the duration over which lift or lateral force can act, slightly diminishing overall movement. Vertical Approach Angle (VAA) reflects the integrated effect of lift, drag, and gravity over the flight path of the ball. A shallower (less negative) VAA indicates that upward Magnus force (from backspin) has been effective in resisting gravity, keeping the ball on a flatter plane. Conversely, a steeper VAA suggests a dominant gravitational and downward Magnus force (as in the case of curveballs or sinkers), indicating reduced lift or increased topspin-induced drop.

6. Engineering Analysis of a Baseball Pitch

A baseball flying through the air is affected by drag and Magnus force as it moves through the fluid, which is complicated to model because of the complex fluid interactions in the air, the baseball's variable surface geometry, etc. Although potential flow predicts zero drag, which is inaccurate for a baseball, the air flowing around the baseball will be assumed as a potential flow for the purpose of more in-depth flow analysis close to the baseball and to get a value for the lift coefficient, C_L. Therefore, the following assumptions can be made to simplify analysis:

- No-slip condition at the ball's surface ($R = a$)
- The air the ball moves through is approximated to be incompressible ($\rho = const.$):
    - This is reasonable because real baseballs travel through a relatively small area (ex. a baseball diamond) where the atmospheric conditions don't vary by a lot and so any changes in the density of air in the area is negligible
    - Also, baseballs tend to travel at fairly subsonic speeds ($Ma < 0.3$, the highest Mach ever number recorded for a baseball was $Ma \approx 0.25$ [4]), so it's even more reasonable to neglect any density changes
- The baseball is approximated as a smooth rotating sphere with fluid (air) moving around it
    - This simplifies the geometry of the baseball by ignoring any imperfections on the surface of a real baseball like the seams, which complicate analysis
- Rotation imparted on the baseball by the pitcher stays constant and is unaffected by fluid interactions ($\omega = const.$)

From the ball's reference as it travels, it appears to stay still while the fluid (air) moves around it. As the fluid flows into and around it, its viscosity causes it to slow down near the ball's surface and "stick" to it, creating an effective zero velocity (i.e. no slip) at the surface. This results in a thin boundary layer created at the ball's surface wherein the fluid inside it has negligible velocity, and the velocity of fluid particles increases further from the boundary layers.

As the fluid flows on the rear surface of the ball, the surface curvature makes the flow expand, which decreases the flow's velocity, increasing the pressure in the process [1].

This effectively creates an adverse (increasing) pressure gradient in the direction of flow, which produces an opposing force on fluid elements as they move around the ball. Eventually, there is a point on the ball's surface where the surface fluid element's momentum reaches 0 $\left(\frac{du}{dy} = 0\right)$, creating a separation point for the boundary layer. Past this point, fluid elements on the surface experience increasing momentum opposite to the

flow direction, creating a backflow which pushes the boundary layers apart, resulting in a low-pressure, turbulent zone called a wake. This resultant wake has higher drag with increasing size and is the main drag contributor on the ball.

The resulting drag acting on a sphere can be approximated using this equation [1]:

$$F_D = \frac{1}{2} C_D \rho A v^2$$

Equation 1: Drag Force on Ball

For the rotating sphere model of a baseball, an experimentally derived value of $C_D = 0.3$ will be used [1].

Additionally, adding rotation to the sphere imparts a Magnus force on it. Taking a cross-sectional area of the sphere parallel to the incoming flow direction, and assuming it as a cylinder face proves useful when explaining the origins of this force. For example, if a clockwise rotation is added to our cylinder, the fluid flowing over top of the cylinder is made faster by the rotation since it's moving in the same direction [2], while the fluid flowing under the cylinder is slowed as it moves against the rotation. This creates asymmetrical boundary layers around the cylinder and so an asymmetrical wake region, which creates a pressure difference between the top and bottom of the cylinder. This altered pressure gradient induces a force on the cylinder perpendicular to the flow direction, upwards in the case of clockwise rotation, called the Magnus force. Conversely, adding counterclockwise direction would produce a force in the opposite direction, downwards.

Obviously, for a sphere the entire flow over the 3D surface must be accounted for, which would look much like the flow over a cylinder but copied around the axis coincident with the flow, due to the sphere's axis symmetry.

The Magnus force for a sphere can be approximated using the following equation [3]:

$$F_M = \frac{1}{2} C_L \rho A v^2$$

Equation 2: Magnus Force on Ball

As the lift coefficient C_L is dependent on the spin and velocity of the ball, an experimental scatter-plot fit line was used to calculate its value [5]:

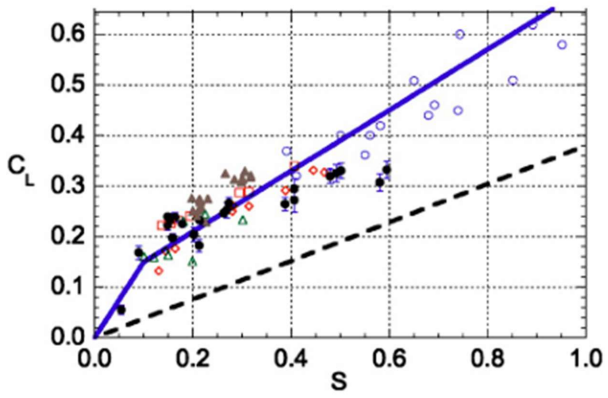

Figure 1: Experimental Results for Lift Coefficient (C_L), shown with the Solid Blue Parameterized Line [5]

It's seen in the figure above that the slope of the parameterized line (blue) changes around $S = 0.1$, which is generally consistent with experimental results [7]. Although the physical reasoning behind this change isn't completely agreed on, it's likely because at a critical Re value for a smooth ball, the C_D decreases suddenly, which is hypothesized to contribute a reverse Magnus effect [5], lowering the overall C_L value.

Nevertheless, the 2 slopes are separated by their respective *S* values, which in turn was used to calculate the lift coefficient of the ball using its velocity and spin rate at any given moment:

Table 1: Calculating the Lift Coefficient based on Spin Rate (S)

If $S < 0.1$	If $S \geq 0.1$
$S = \frac{R\omega}{v}$ $C_L = 1.5S$	$S = \frac{R\omega}{v}$ $C_L = \frac{2}{3}(S - 0.1) + 0.15$

6.1 Free Body Diagram of a Baseball in Flight

Taking the assumptions and force approximations above, a 3D FBD (Free Body Diagram) can be made for a baseball flying through the air:

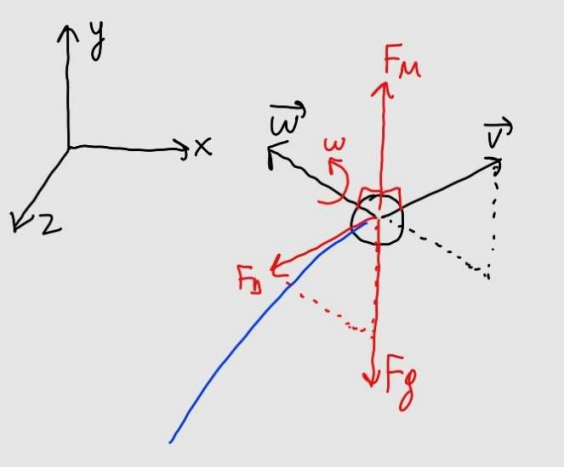

Figure 2: 3D FBD of Baseball in Flight (Blue line is the Ball's Trajectory for Reference)

As can be seen in the diagram, the 3 main forces that act on the ball while it travels are the force due to gravity, F_g, the drag force, F_D, and the Magnus force, F_M. The drag on the ball acts opposite to the velocity and can be represented using *Equation 1*. The Magnus force acts in the $\vec{\omega} \times \vec{v}$ direction, represented by *Equation 2*.

Finally, the gravitational force pulls the baseball downwards, represented by the following equation:

$$F_g = mg$$

Equation 3: Gravitational Force

7. Model Development and Methodology

7.1 Development of a Simplified Baseball Trajectory Model

To predict the trajectory of a baseball using the model for Magnus effect, a force balance of the ball at any point in time must be made using *Equations 1-3* along with initial pitch and trajectory conditions.

A table of the model conditions can be found below:

Table 2: Model Parameters

Parameter	Function
Extension	Used to calculate the distance to home plate
Pitch Height	Informs initial height of pitch
Plate Height	Informs the height at which a pitch crosses the plate
Velo	Pitch Velocity: Necessary for Modelling
Active Spin	Defined as the Percentage of Spin contributing to motion as percentage, artificially deflates spin rate to account motion about the gyroscopic axis (incurring motion in the travelled direction without break or drop)
Spin	Spin Rate: Necessary for Modelling
Spin Axis	Defines the portion of spin contributing to the Magnus effect in different cartesian directions
Vertical Movement	Empirical MLB value of the difference between the drop of the actual pitch as compared to a non-spinning baseball
Horizontal Break	Empirical MLB value of the difference between the break of the actual pitch as compared to a non-spinning baseball

As the force values and the velocity of the ball vary as the ball travels through the air, it is most efficient to employ a numerical solving method to calculate the forces, velocities, and accelerations on the ball at every point along the ball's path using an iteration time Δt.

At time $t = 0$, the ball has defined position and velocity vectors, along a known target position in the x-y frame, but a known pitch angle to solve these boundary conditions. First, an arbitrarily low angle is selected, and then the velocity vectors are used to calculate the drag and magnus forces on the ball. These forces can be translated to acceleration in each cartesian direction by the mass of the baseball, at which point a Eulerian integration scheme is employed to approximate the resulting velocity vectors, given by

$$\Delta v = a \cdot \Delta t$$

With these updated vectors, a secondary Eulerian integration is then applied to solve for the updated position of the baseball, where:

$$\Delta x = v \cdot \Delta t$$

At this point, the updated velocities are used to recalculate the force vectors, and the process repeats until the ball has crossed home plate. Upon crossing home plate, the ball height is cross referenced with the boundary condition, and the simulation rerun with an increased angle. This process repeats until the crossing height is greater than the boundary condition, at which point the 'actual angle' is extrapolate.

The loop is run one last time with no magnus effect and concludes when the ball crosses home plate. The horizontal position vector from the full simulation at the actual angle represents the break incurred by spin, and the difference between the crossing heights with and without magnus force at the actual angle the drop, which can be compared to MLB data.

7.2 Comparing to Experimental Pitch Data

To develop a suitable sample size for the model, the season averages for each input were taken for different pitchers. Pitchers selected in the 4-Seam category include those that pitched more than 500 4-Seamers in the 2024 season, and in the curveball category a minimum of 200 pitches. This leads to a sample size of 149 4-Seamers and 88 curveballs.

8. Results

8.1 Rising Fastball Results

When plotting the theoretical trajectory of the fastball pitches with and without the Magnus force contribution, the following graph is made:

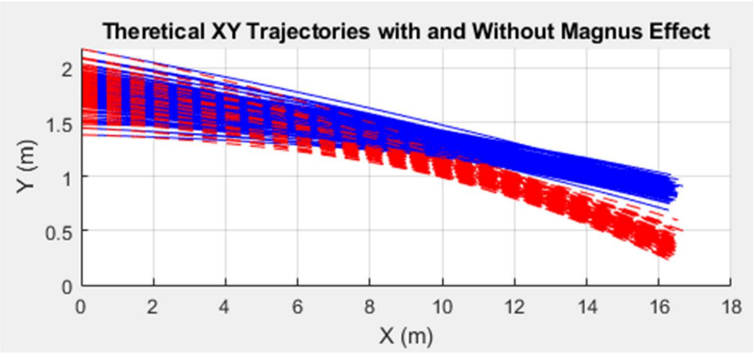

Figure 3: Theoretical Fastball Trajectory with Magnus Effect (Blue lines) and without (Red lines)

The results from the figure above are consistent with predictions, as the pitches without the contribution of the Magnus effect (red) fall quicker, since the Magnus effect is no longer providing any lift.

Comparing the break (Δx) and drop (Δy) of each fastball pitch's final placement relative to the final placement of the empirical pitch results in the following graph:

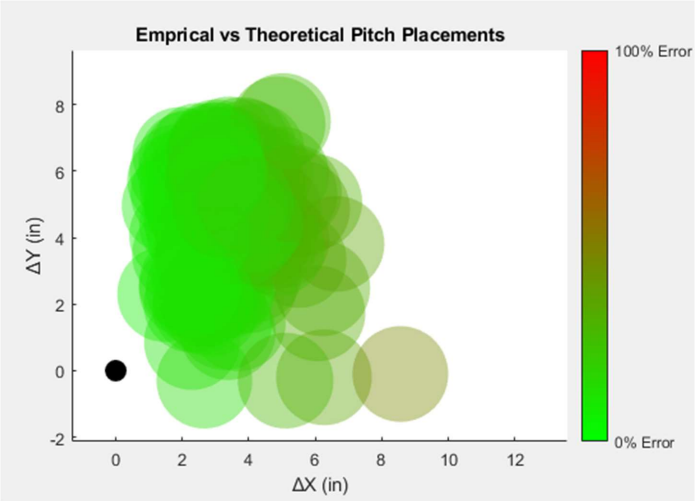

Figure 4: Experimental vs Theoretical Pitch Placements for Fastballs

The figure above shows that the theoretical model is relatively accurate for fastballs as most of the pitches line up closely with empirical results, though there are a couple of outliers with errors approaching 40-50% (the brownish spots on the right edges of the green mass).

8.2 Curveball Results

When plotting the theoretical trajectory of the curveball pitches with and without the Magnus force contribution, the following graph is made:

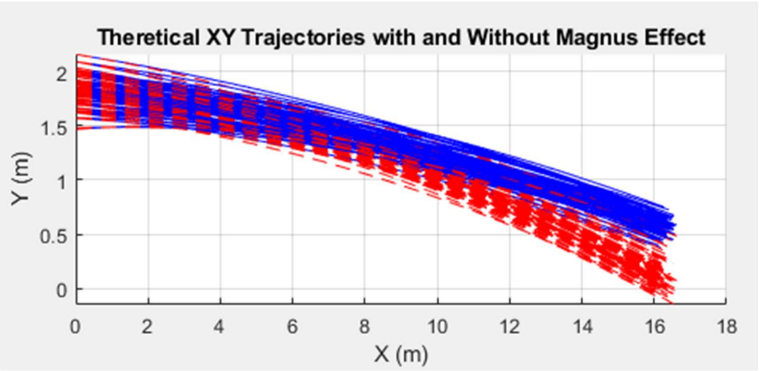

Figure 5: Theoretical Curveball Trajectory with Magnus Effect (Blue lines) and without (Red lines)

While the results in the figure above are consistent with predictions once again, since removing the effect of Magnus force makes the baseballs fall quicker without its additional lift, the curveballs seem to end up at a lower position than the fastballs.

This is consistent with empirical observations and is mostly due to the fact that curveballs are thrown with a focus on greater angular velocity to make the ball break more (i.e. dip more in flight) in order to make in harder to hit. Curveballs tend to be thrown with topspin in order to create a higher-pressure zone on top of the ball to make it drop further down as it travels [6], which would explain why the curveballs generally end up at a lower position than the fastballs. This focus on imparting spin and not power also makes curveballs inherently slower since the pitcher doesn't focus as much on imparting greater power on the ball and thereby making it faster, which gives gravity more time to act on the ball and push it towards the ground.

Comparing the break (Δx) and drop (Δy) of each curveball pitch's final placement relative to the final placement of the empirical pitch results in the following graph:

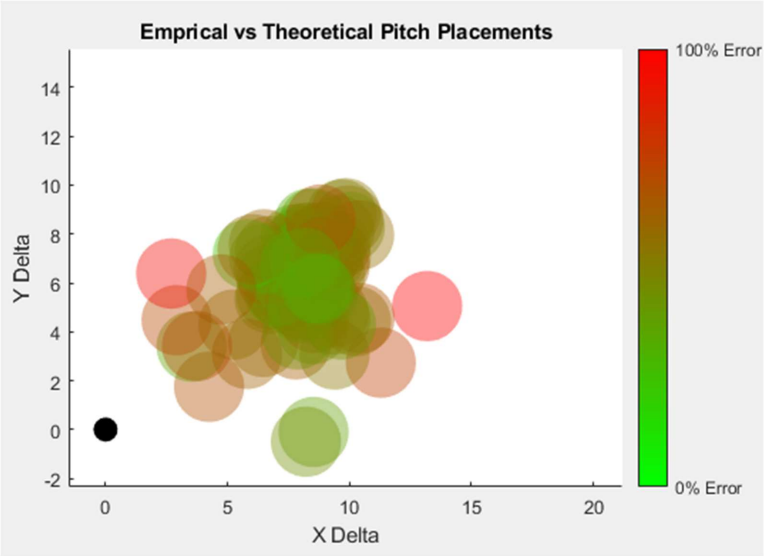

Figure 6: Experimental vs Theoretical Pitch Placements for Curveballs

From the figure above, it's seen immediately that there is more error involved with the curveball model than the fastball one. This can be explained in part because the C_L from *Figure 1* was calculated for fastballs specifically [5], making it inaccurate for representing lift with respect to curveballs.

9. Justification and Limitations of Model

Overall, as shown above, the theoretical model holds decently well with MLB results for rising fastballs but fails to properly account for the break and rise experienced by curveballs. However, the lift coefficient C_L can be tuned in order to investigate if the accuracy of the curveball model increases with a properly tuned C_L value.

9.1 Tuning of Lift Coefficient

Since fastballs inherently have less spin on them than curveballs, it's reasonable to assume they would have a lower C_L value. This is backed up by *Figure 1,* where it's seen that C_L increases with increasing spin.

Therefore, the C_L value used for the curveball model can be increased in increments of 0.01 to see if the model becomes more accurate. When running the model with $C_L = [0.15{,}2]$ as a test, it was observed that $C_L = 1.67$ resulted in a curveball model with the greatest accuracy:

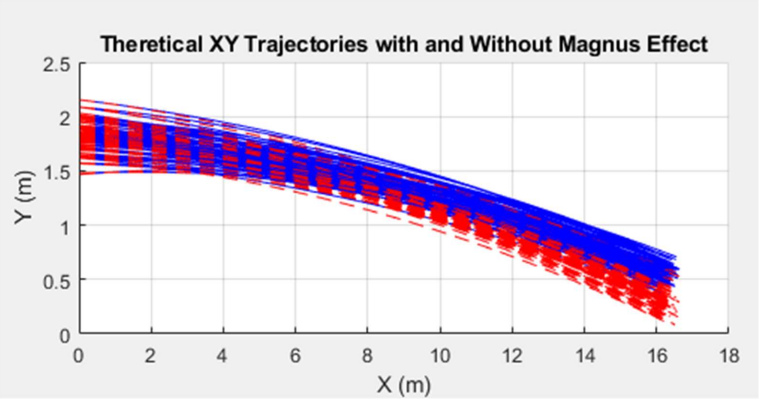

Figure 7: Theoretical Curveball Trajectory with Magnus Effect (Blue lines) and without (Red lines) using an Optimized Lift Coefficient (C_L=1.67)

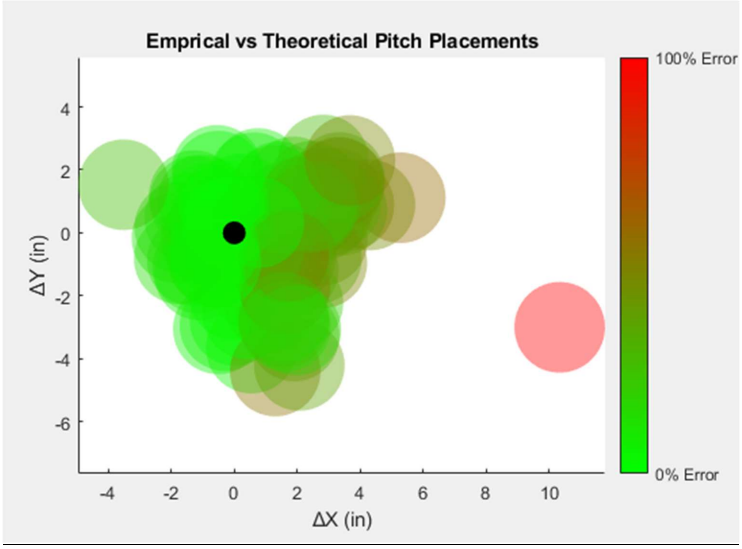

Figure 8: Experimental vs Theoretical Pitch Placements for Curveballs with Optimized Lift Coefficient (C_L=1.67)

From the figure above, it's concluded that adjusting for an optimal coefficient of $C_L = 1.67$ results in a decently accurate model for baseball trajectory, although it's important to note that it's still slightly less accurate than the fastball model (*Figure 4*), proven by the presence of more brownish circles (i.e. more pitches of higher error with respect to empirical results).

This is likely due to the increased spin on curveballs contributing to more complex fluid interactions with the baseball, making their trajectory more difficult to predict as opposed to fastballs, which also tend to have higher velocities. It's important to note that the wake that forms behind a baseball is a region of turbulent airflow, which isn't fully accounted for with present-day fluid dynamics solutions, resulting in drag and Magnus force approximations that require a fair bit of simplification, but this problem is compounded with baseballs that spin more (i.e. curveballs) since the resultant wake is asymmetrical and even more complex, proving even more that curveballs are inherently more difficult to model.

10. Conclusion

To summarize, the fluid dynamics surrounding a pitched baseball and its respective drag and Magnus force contributions was investigated in order to make a theoretical model for its trajectory, which was very accurate for fastballs and less so for curveballs. The background of the sport of baseball and the development of its analysis and associated terminology were discussed. The behaviour of air flowing into and around the baseball as it flies was discussed in an Engineering context, and the theoretical drag and Magnus forces imparted on the baseball were calculated using experimental data. A 3D free body diagram of a baseball travelling through the air was made to obtain force/kinematic equations at any point in time between being thrown and hit by a bat, and the resulting equations were used to make a numerical solution for the trajectory of a baseball using empirical pitching parameters from MLB statistics. This numerical solution was then applied in MATLAB to predict the theoretical trajectory of different kinds of pitches, and these were in turn compared to their empirical counterparts.

11. References

[1] M. Dasilva, "Drag on a Baseball," NASA Glenn Research Center, 11 September 2023. [Online]. Available: https://www1.grc.nasa.gov/beginners-guide-to-aeronautics/drag-on-a-baseball/#drag-coefficient-of-a-baseball. [Accessed 4 April 2025].

[2] N. Hall, "Lift of Rotating Cyclinder," NASA Glenn Research Center, 13 May 2021. [Online]. Available: https://www.grc.nasa.gov/www/k-12/airplane/cyl.html. [Accessed 4 April 2025].

[3] M. Dasilva, "Lift of a Baseball," NASA Glenn Research Center, 17 June 2022. [Online]. Available: https://www1.grc.nasa.gov/beginners-guide-to-aeronautics/lift-of-a-baseball/. [Accessed 4 April 2025].

[4] "Fastest baseball pitch (male)," Guiness World Records, 2010 September 2010. [Online]. Available: https://www.guinnessworldrecords.com/world-records/fastest-baseball-pitch-(male). [Accessed 4 April 2025].

[5] A. M. Nathan, "The effect of spin on the flight of a baseball," 13 October 2007. [Online]. Available: https://baseball.physics.illinois.edu/AJPFeb08.pdf. [Accessed 4 April 2025].

[6] R. Tobin, "How Do Curve Balls, Cutters, Sinkers, and Sweepers Work?," TuftsNow, 2024 August 22. [Online]. Available: https://now.tufts.edu/2024/08/22/how-do-curve-balls-cutters-sinkers-and-sweepers-work. [Accessed 4 April 2025].

[7] "Statcast Search," MLB Advanced Media, [Online]. Available: https://baseballsavant.mlb.com/statcast_search. [Accessed 4 April 2025].

12. Appendix

12.1 MATLAB Code

```
clear all; close all; clc;


m = 0.145;
R = 0.0366;
A = pi*R^2;
rho = 1.29;
g = 9.81;
Cd = 0.3;


data = readtable('curves_final.xlsx');
values = table2array(data);
deltas = zeros(size(data,1),6);

figure;
hold on;
xlabel('X (m)');
ylabel('Y (m)');
title('Theretical XY Trajectories with and Without Magnus Effect)');
grid on;

for i = 1:size(data,1)

    v0 = values(i,4) * 0.44704;
    spin_rate = values(i,5) * (values(i,6) / 100);
    spin_angle = values(i,9);
    travel_plate = (60 - values(i,1)) * 0.3048;
    rise_release = values(i,2) * 0.3048;
    rise_target = values(i,3) * 0.3048;

    omega_rise = cosd(spin_angle) * spin_rate * (2*pi/60);
    omega_break = sind(spin_angle) * spin_rate * (2*pi/60);

    theta_range = linspace(-5, 25, 200);
    calcd_angle = 0;
    min_error = inf;
    calcd_px = [];
    calcd_py = [];
    calcd_pz = [];

    for theta_deg = theta_range
        theta_rad = deg2rad(theta_deg);
        mag_v_travel = v0*cos(theta_rad);
        mag_v_rise = v0*sin(theta_rad);
        mag_v_break = 0;
        mag_p_trav0 = 0;
        mag_p_rise0 = rise_release;
        mag_p_break0 = 0;
```

```
mag_p_trav = [];
mag_p_rise = [];
mag_p_break = [];


for t = 0:0.001:2
    v = sqrt(mag_v_travel^2 + mag_v_rise^2 + mag_v_break^2);

    % Drag force
    Fd_mag = 0.5*rho*Cd*A*v^2;
    Fd_mag_travel = -Fd_mag*mag_v_travel/v;
    Fd_mag_rise = -Fd_mag*mag_v_rise/v;
    Fd_mag_break = -Fd_mag*mag_v_break/v;

    % Magnus force
    s_rise = abs(R*omega_rise/v);
    s_break = abs(R*omega_break/v);

    if s_rise < 0.1
        Cl_Rise = s_rise*1.5/1.67;
    else
        Cl_Rise = ((s_rise-0.1)*(2/3) + 0.15)/1.67;
    end

    if s_break < 0.1
        Cl_break = s_break*1.5/1.67;
    else
        Cl_break = ((s_break-0.1)*(2/3) + 0.15)/1.67;
    end

    Fm_Rise = 0.5*rho*Cl_Rise*A*v^2;
    Fm_Break = 0.5*rho*Cl_break*A*v^2 * sign(mag_v_travel);

    mag_v_travel = mag_v_travel + Fd_mag_travel/m*0.001;
    mag_v_rise = mag_v_rise + (Fd_mag_rise + Fm_Rise)/m*0.001 - g*0.001;
    mag_v_break = mag_v_break + (Fd_mag_break + Fm_Break)/m*0.001;

    mag_p_trav0 = mag_p_trav0 + mag_v_travel*0.001;
    mag_p_rise0 = mag_p_rise0 + mag_v_rise*0.001;
    mag_p_break0 = mag_p_break0 + mag_v_break*0.001;

    mag_p_trav(end+1) = mag_p_trav0;
    mag_p_rise(end+1) = mag_p_rise0;
    mag_p_break(end+1) = mag_p_break0;

    if mag_p_trav0 >= travel_plate
        error = abs(mag_p_rise0 - rise_target);
        if error < min_error
            min_error = error;
            calcd_angle = theta_deg;
            calcd_px = mag_p_trav;
            calcd_py = mag_p_rise;
            calcd_pz = mag_p_break;
        end
        break;
```

```
            end

            if mag_p_rise0 < 0
                break;
            end
        end
    end

    plot(calcd_px, calcd_py, 'b-', 'DisplayName', 'With Spin');

        theta_rad = deg2rad(calcd_angle);
        grav_v_travel = v0*cos(theta_rad);
        grav_v_rise = v0*sin(theta_rad);
        grav_v_break = 0;
        grav_p_trav0 = 0;
        grav_p_rise0 = rise_release;
        grav_p_break0 = 0;

        grav_p_trav = [];
        grav_p_rise = [];
        grav_p_break = [];

        for t = 0:0.001:2
            v = sqrt(grav_v_travel^2 + grav_v_rise^2 + grav_v_break^2);

            Fd_grav = 0.5*rho*Cd*A*v^2;
            Fd_grav_travel = -Fd_grav*grav_v_travel/v;
            Fd_grav_rise = -Fd_grav*grav_v_rise/v;
            Fd_grav_break = -Fd_grav*grav_v_break/v;

            grav_v_travel = grav_v_travel + Fd_grav_travel/m*0.001;
            grav_v_rise = grav_v_rise + (Fd_grav_rise)/m*0.001 - g*0.001;
            grav_v_break = grav_v_break + (Fd_grav_break)/m*0.001;

            grav_p_trav0 = grav_p_trav0 + grav_v_travel*0.001;
            grav_p_rise0 = grav_p_rise0 + grav_v_rise*0.001;
            grav_p_break0 = grav_p_break0 + grav_v_break*0.001;


            grav_p_trav(end+1) = grav_p_trav0;
            grav_p_rise(end+1) = grav_p_rise0;
            grav_p_break(end+1) = grav_p_break0;


            if grav_p_trav0 >= travel_plate
               break
            end

        end

    deltas(i,1) = values(i,10);
    deltas(i,2) = -values(i,11);
    deltas(i,3) = (calcd_py(1,size(calcd_py,2)) - grav_p_rise(1,size(grav_p_rise,2)))
* 39.37;
```

```
    deltas(i,4) = (calcd_pz(1,size(calcd_pz,2)) -
grav_p_break(1,size(grav_p_break,2))) * 39.37;
    deltas(i,5) = deltas(i,3) - deltas(i,2);
    deltas(i,6) = deltas(i,4) - deltas(i,1);
    deltas(i,7) = abs(100* (deltas(i,3) - deltas(i,2)) / deltas(i,3));
    deltas(i,8) = abs(100* (deltas(i,4) - deltas(i,1)) / deltas(i,4));

    fprintf('Pitch %d: Required launch angle = %.2f°\n', i, calcd_angle);

    plot(grav_p_trav, grav_p_rise, 'r--', 'DisplayName', 'Without Spin');

end

daspect([3 1 1]);

% Define circle parameters
radius = 0.0366;       % Radius in meters
center = [0, 0];       % Center coordinates [x, y]
theta = linspace(0, 2*pi, 100);  % Angle values for smooth circle

% Generate circle coordinates
x = center(1) + radius * cos(theta);
y = center(2) + radius * sin(theta);
data_column7 = linspace(0, 100, 100)';
normalized_data = data_column7 / 100;
custom_colormap = [linspace(0,1,100)', linspace(1,0,100)', zeros(100,1)];

x = deltas(:, 5);
y = deltas(:, 6);
c = deltas(:, 7);



x = deltas(:, 5);
y = deltas(:, 6);
c = deltas(:, 7);
c_norm = c / 100;
cmap = [linspace(0,1,100)', linspace(1,0,100)', zeros(100,1)]; % green to red

figure; hold on; axis equal;

for i = 1:length(x)
    color_idx = max(1, min(100, round(c_norm(i) * 99) + 1));
    fill_color = cmap(color_idx, :);
    theta = linspace(0, 2*pi, 50);
    cx = 39.37 * R * cos(theta) + x(i);
    cy = 39.37 * R * sin(theta) + y(i);
    fill(cx, cy, fill_color, 'EdgeColor', 'none', 'FaceAlpha', 0.4);
end

plot(0, 0, 'ko', 'MarkerSize', 12, 'MarkerFaceColor', 'k'); % black circle at origin
xlabel('ΔX (in)');
ylabel('ΔY (in)');
title('Emprical vs Theoretical Pitch Placements');
colormap(cmap);
```

```
cb = colorbar;
cb.Ticks = [0, 1];
cb.TickLabels = {'0% Error', '100% Error'};
```

12.2 Data Sets

See attached files ‘4-Seam Data.xlsx’ and ‘Curveball Data.xlsx’.